Polish J. Chem., **76**, 309–324 (2002)

One-, Two- and Non-Coordinated CrO_4^{2-} Entity in the Nickel(II) Complexes. Structural and Spectroscopic Investigation*

by A. Pietraszko[1], W. Bronowska[2], A. Wojciechowska[3], Z. Staszak[4] and M. Cieślak-Golonka[3]**

[1]*Institute of Low Temperature and Structure Research, Polish Academy of Sciences, Okólna 2, 59-950 Wrocław, Poland*
[2]*Institute of Physics, Wrocław University of Technology*
[3]*Institute of Inorganic Chemistry and Metallurgy of Rare Elements, Wrocław University of Technology*
[4]*Faculty of Computer Science and Management, Wrocław University of Technology, Wybrzeże Wyspiańskiego 27, 50-370 Wrocław, Poland*

(Received July 10th, 2001; revised manuscript October 1st, 2001)

A systematic investigation of the chromate ion in [Ni(II)-(2,2′-bpy)-CrO_4^{2-}] systems has been carried out. The effect of the Ni(II) ion and the organic ligand on the mode of the chromate position in the $[Ni(bpy)_3]CrO_4 \cdot 7.5H_2O$ (**1**), $[Ni(bpy)_2(OCrO_3)(H_2O)] \cdot 5H_2O$ (**2**) and *catena*-(μ-CrO_4-*O,O′*)$[Ni(bpy)(H_2O)_2] \cdot 2H_2O$ (**3**) complexes has been shown. $[Ni(bpy)_3]CrO_4 \cdot 7.5H_2O$ crystals (**1**) have a monoclinic symmetry with space group *C*2/*c* and 8 chemical units, forming a unit cell with a = 13.641(3) Å, b = 22.939(5) Å, c = 23.351(5) Å and β = 104.69(3) deg, whereas the $[Ni(bpy)_2(OCrO_3)(H_2O)] \cdot 5H_2O$ crystals (**2**) have a monoclinic symmetry with space group $P2_1/c$ and 4 chemical units per unit cell with a = 10.854(2) Å, b = 22.665(5) Å, c = 10.623(2) Å and β = 108.93(3) deg at room temperature. The chromate ion in **1** is not coordinated to the nickel(II) ion. The geometry around the Cr(VI) atom is pseudotetrahedral. Untypical for the chromate ion monodentate coordination has been found in the complex $[Ni(bpy)_2(OCrO_3)(H_2O)] \cdot 5H_2O$. The chromate position has been also elucidated from the digitally resolved IR spectra. The coordination of the chromate ion in **2** and **3** was also observed for the single crystal at 4 K, in reflectance and solution electronic spectra through the appearance of a new transition at *ca.* 15000 cm^{-1}. The full characterization of the chromophores present in the complexes: NiN_6, NiN_4O_2, NiN_2O_4 and NiO_6 have been obtained on the basis of the detailed analysis of the electronic spectra at 4 K (Gaussian deconvolution followed by digital filtration).

Key words: crystal structure, Ni(II) complexes, chromate ion, electronic spectra

Extensive data exist in literature on the redox pathways of the carcinogenic Cr(VI) anion and the interaction of its metabolites, *i.e.* Cr(V), Cr(IV) and Cr(III) with DNA [1–5]. However, in contrast to simple chromate salts, only a few data on the biological properties of the metal ion complexes, containing the Cr(VI) ion, have been reported [6–7]. In the bacterial tests on the Cu(II) chromate complexes with some ni-

---

* Dedicated to the memory of Professor Krzysztof Pigoń.

** To whom correspondence should be addressed: Phone: (048) 07134335028;
E-mail address: adam@int.pan.wroc.pl

trogen donor ligands, depending on the chemical composition of the $Cu_xL_yCrO_4$ complexes (L-heterocyclic base), various degree of genotoxicity, decreasing in comparison to control simple chromate, have been found [6–7]. The lowering of the mutagenic activity was explained by the mode of the chromate ion binding to the metal-organic ligand core [2]. Thus, the symmetry of the Cr(VI) species forming may influence, *e.g.* the effectivity of the membrane crossing.

The aim of this study was a systematic investigation of geometry changes of the chromate ion, depending upon the condition of the experiment. Particularly, the effect of the M:L ratio in the [Ni(II)-bpy-CrO_4^{2-}] system on the CrO_4^{2-} position in the isolated species has been investigated. The first two members of the system, *i.e.* $Nibpy_x^{2+}$ complex ions (x = 1, 2, 3), which may play here a modifying role with respect to the CrO_4^{2-}, were studied intensively earlier [8–18]. Having in mind the biological effects, we were especially interested in the stability of the isolated species in the solution.

EXPERIMENTAL

Preparation of [Ni(bpy)$_3$]CrO$_4$·7.5H$_2$O (1) and catena-(μ-CrO$_4$-O,O′)[Ni(bpy)(H$_2$O)$_2$]·2H$_2$O (3): Complexes were prepared as described in [19].

Preparation of [Ni(bpy)$_2$(OCrO$_3$)(H$_2$O)]·5H$_2$O (2): A methanolic solution of 2,2′-bipyridine (20 cm^3, 0.75 M) was added upon stirring to the K_2CrO_4 water solution (30 cm^3, 0.25 M). After 15 min this was mixed with 30 cm^3 of the 0.25 M nickel chloride (sulfate, nitrate). The resulting solution of red brown color was allowed to stand in air and after 24 h gave an olive powder precipitate, *i.e.* complex **3**. After filtration of **3** the solution was slightly evaporated at room temperature and allowed to remain for a minimum of 7 days. The dark olive crystals obtained were filtered, washed several times with water and finally dried in a vacuum desiccator over P_2O_5. Anal. Calc $C_{20}H_{28}CrN_4O_{10}Ni$: Ni, 9.84; Cr, 8.81; C, 40.71; N, 9.49; H, 4.77. Found: Ni, 8.8; Cr, 8.35; C, 40.38; N, 9.21; H, 4.57. Elemental analyses were performed with the Kupman (C, H, N) and ICP (Cr, Ni) methods.

X-ray crystallography and structure solution: The single-crystal measurements were carried out on the four circle X-ray KM4-CCD diffractometer (KUMA DIFFRACTION Company) with graphite-monochromated MoK_α radiation (λ = 0.71073 Å). X-ray intensity data were collected at 300 K in 5 runs on 120° omega angle using a step 0.5° and 25 s exposures for one image. 15879 reflections of [Ni(bpy)$_3$]CrO$_4$·7.5H$_2$O (**1**) and 13347 reflections of [Ni(bpy)$_2$(OCrO$_3$)(H$_2$O)]·5H$_2$O (**2**) were recorded to a resolution 0.78 Å, which merged to give a total of 5225 and 4169 unique reflections, respectively. Empirical absorption correction was applied for observed reflections and extinction correction was introduced in the refinement. The structures of crystals **1** and **2** were solved by direct methods using the SHELXS-97 program [20]. The positions of hydrogen atoms were determined from difference Fourier maps. Refinement was carried out using SHELXL-97 [20]. The initial lattice parameters were calculated from 120 reflections and the final lattice parameters were refined for all reflections with $I > 2$ sigma(I).

Magnetic measurements and vibrational spectroscopy: Magnetic measurements were carried out at 293 K by the Gouy method using Hg[Co(SCN)$_4$] as calibrant. Infrared and FIR spectra were recorded on a Perkin Elmer 1600 and FT-IR Perkin Elmer 2000 spectrophotometers, respectively. The band analysis was performed using the variable digital filter method [21–24].

Electronic spectra measurements: A Cary 500 Scan UV-Vis-NIR spectrophotometer was used for spectra recording. The spectra of the formamide solutions were of the concentrations: 5×10^{-3} M for **1** and **2**. Additionally, the spectra of the hydrated Ni(II) salts (sulfate, chloride and nitrate) in formamide (5×10^{-3} M) were investigated for comparison. (For **3** because of low solubility only the reflectance spectrum was measured). Single crystal low-temperature (4 K) absorption spectra were recorded in the range 9000–20500 cm^{-1}, using the Cryostat Optistat CF (Oxford) open-cycle helium system. A two-step procedure was performed for the resolution of the spectra: (i) – the variable digital filtration (to obtain the ap-

proximate values of the band positions) [21–24], (ii) – the deconvolution of the spectral contour into Gaussian components (to obtain the exact values of the band intensity, half width and position). The processes of deconvolution were performed by modification of non-linear least squares algorithm [25–27]. For d-d bands the data obtained were used to calculate the crystal field Dq, Ds, Dt parameters and Racah B parameter. In the calculation the Perumareddi matrices [28–29] (without spin-orbit coupling parameter) for spin allowed transition were used. The parameters were found by minimizing (SIMPLEX algorithm) the root mean square error between experimental energies (taken from deconvolution) and theoretical energies (taken from the Perumareddi matrices [28–29]).

RESULTS AND DISCUSSION

Description of the structures: The details of data collection and refinement are shown in Table 1. The $[Ni(bpy)_3]CrO_4 \cdot 7.5H_2O$ crystals **1** have a monoclinic symmetry with space group *C*2/*c* and 8 chemical units forming a unit cell at room temperature, whereas the $[Ni(bpy)_2(OCrO_3)(H_2O)] \cdot 5H_2O$ crystals **2** have a monoclinic symmetry with space group *P*2(1)/*c* and 4 chemical units per unit cell (Table 1). Selected interatomic distances and angles of crystal **1** and **2** are shown in Table 2. The arrangement of $[Ni(bpy)_3]^{2+}$ complex ions, chromate ions and molecules of water of crystallization in **1** is similar to that in $[Ni(bpy)_3]SO_4 \cdot 7.5H_2O$ [30]. Two non-equivalent groups $[Ni(1)(bpy)_3]^{2+}$ and $[Ni(2)(bpy)_3]^{2+}$ (Fig. 1) are built into the hydrogen-bonded carcass, which is composed entirely of water molecules and chromate ions. The chromate ion is not coordinated to the nickel(II) ion. The geometry around the Cr(VI) atom is pseudotetrahedral, where Cr–O bond lengths are in the range 1.598(3)–1.672(5) Å. The O(3A) and O(3B) atoms of CrO_4^{2-} and the water O(8) atoms statistically occupy their position with k = 0.5, which means that the chromate ions undergo reorientational motion between two equilibrium arrangements with equal probability (Fig. 2). The large values of the anisotropic temperature factors of all oxygen atoms indicate that the structure of the crystals **1** is dynamically disordered.

Table 1. Selected crystallographic data for $[Ni(bpy)_3]CrO_4 \cdot 7.5H_2O$ (**1**) and $[Ni(bpy)_2(OCrO_3)(H_2O)] \cdot 5H_2O$ (**2**).

	1	**2**
empirical formula	$NiCrC_{30}H_{39}N_6O_{11.5}$	$NiCrC_{20}H_{28}N_4O_{10}$
fw	778.38	595.16
T(K)	293(2)	293(2)
λ (MoKα) (Å)	0.71073	0.71073
space group	*C*2/*c*	$P2_1/c$
a (Å)	13.641(3)	10.854(2)
b (Å)	22.939(5)	22.665(5)
c (Å)	23.351(5)	10.623(2)
α (°)	90	90
β (°)	104.69(3)	108.93(3)

Table 1 (continuation)

γ (°)	90	90
V (Å)^3	7068(3)	2472.0(8)
Z	8	4
d_{calcd} (g/cm^3)	1.463	1.599
R_1[a]	0.070	0.053
wR_2[b]	0.145	0.100

[a]$R_1 = \Sigma||F_o| - |F_c||/\Sigma|F_o|$. [b]$wR_2 = \{\Sigma[w(F_o^2 - F_c^2)^2]/\Sigma[w(F_o^2)^2]\}^{1/2}$.

Table 2. Selected bond lengths (Å) and angles (deg) in crystals $[Ni(bpy)_3]CrO_4 \cdot 7.5H_2O$ (**1**) and $[Ni(bpy)_2(OCrO_3)(H_2O)] \cdot 5H_2O$ (**2**).

(1)	Ni(1)–N(1A)	2.0888(17)	Ni(2)–N(1E)	2.0744(16)
	Ni(1)–N(1A)#3	2.0888(17)	Ni(2)–N(1E)#3	2.0744(16)
	Ni(1)–N(1B)#3	2.0936(16)	Ni(2)–N(1F)	2.0869(18)
	Ni(1)–N(1B)	2.0936(16)	Ni(2)–N(1F)#3	2.0869(18)
	Ni(1)–N(1C)	2.0948(16)	Ni(2)–N(1D)#3	2.0927(15)
	Ni(1)–N(1C)#3	2.0948(16)	Ni(2)–N(1D)	2.0927(15)
		Cr(1)–O(2A)	1.602(3)	
		Cr(1)–O(3B)	1.598(3)	
		Cr(1)–O(4A)	1.609(2)	
		Cr(1)–O(1A)	1.624(2)	
		Cr(1)–O(3A)	1.672(5)	
	N(1A)–Ni(1)–N(1A)#3	92.90(9)	O(2A)–Cr(1)–O(3B)	94.24(17)
	N(1A)–Ni(1)–N(1B)#3	78.36(6)	O(2A)–Cr(1)–O(4A)	107.70(13)
	N(1A)–Ni(1)–N(1B)	94.39(6)	O(3B)–Cr(1)–O(4A)	124.50(15)
	N(1A)–Ni(1)–N(1C)	94.86(7)	O(2A)–Cr(1)–O(1A)	109.05(16)
	N(1A)–Ni(1)–N(1C)#3	169.13(6)	O(3B)–Cr(1)–O(1A)	109.35(15)
			O(4A)–Cr(1)–O(1A)	110.17(12)
	N(1E)–Ni(2)–N(1F)	95.30(6)	O(2A)–Cr(1)–O(3A)	127.10(2)
	N(1E)–Ni(2)–N(1D)	93.90(6)	O(3B)–Cr(1)–O(3A)	37.2(2)
	N(1E)–Ni(2)–N(1E)#3	94.15(9)	O(4A)–Cr(1)–O(3A)	93.9(2)
	N(1E)–Ni(2)–N(1F)#3	78.90(5)	O(1A)–Cr(1)–O(3A)	107.37(19)
	N(1E)–Ni(2)–N(1D)#3	169.77(6)	Cr(1)–O(1A)–O(2A)	35.19(10)
	Symmetry transformation used to generate equivalent atoms: #3 –x, y, –z + 1/2			
(2)	Ni(1)–N(1D)	2.068(3)	Cr(1)–O(1)	1.678(2)
	Ni(1)–N(1B)	2.071(3)	Cr(1)–O(2)	1.602(3)
	Ni(1)–N(1C)	2.076(3)	Cr(1)–O(3)	1.642(3)
	Ni(1)–N(1A)	2.083(3)	Cr(1)–O(4)	1.629(3)
	Ni(1)–O(1A)	2.124(3)	Ni(1)–O(1)–Cr(1)	3.724(3)
	Ni(1)–O(1)	2.046(3)		
	N(1A)–Ni(1)–N(1D)	94.78(11)	Cr(1)–O(1)–Ni(1)	126.69(13)
	N(1A)–Ni(1)–N(1B)	78.79(11)	O(2)–Cr(1)–O(4)	110.90(16)
	N(1A)–Ni(1)–N(1C)	92.08(12)	O(2)–Cr(1)–O(3)	109.71(15)
	N(1A)–Ni(1)–O(1A)	176.41(10)	O(4)–Cr(1)–O(3)	108.58(14)
	N(1A)–Ni(1)–O(1)	91.80(11)	O(2)–Cr(1)–O(1)	109.37(14)
	N(1D)–Ni(1)–O(1)	93.31(11)	O(4)–Cr(1)–O(1)	109.98(13)
	N(1B)-Ni(1)-O(1)	91.34(10)	O(3)-Cr(1)-O(1)	108.28(13)
	O(1)-Ni(1)-O(1A)	90.28(10)		

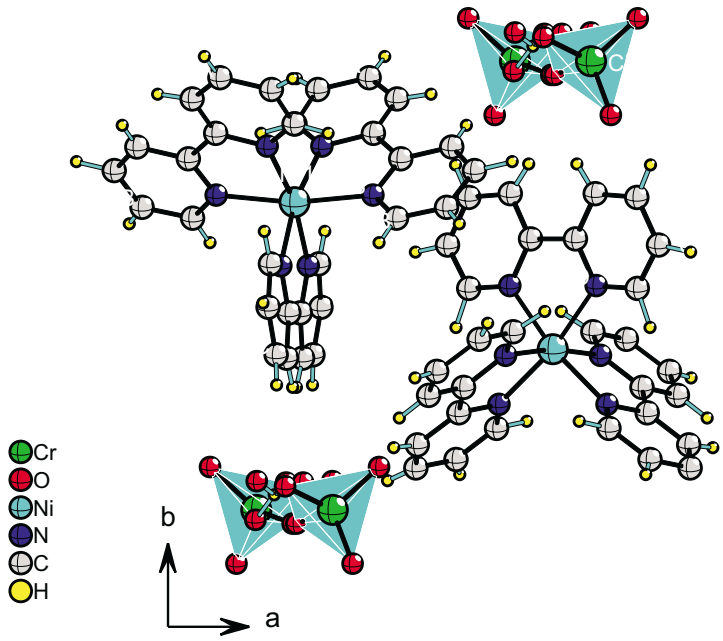

Figure 1. A perspective view of the non-equivalent groups $[Ni(1)(bpy)_3]^{2+}$ and $[Ni(2)(bpy)_3]^{2+}$ and the chromate ions in $[Ni(bpy)_3]CrO4{\cdot}7.5H_2O$ (**1**).

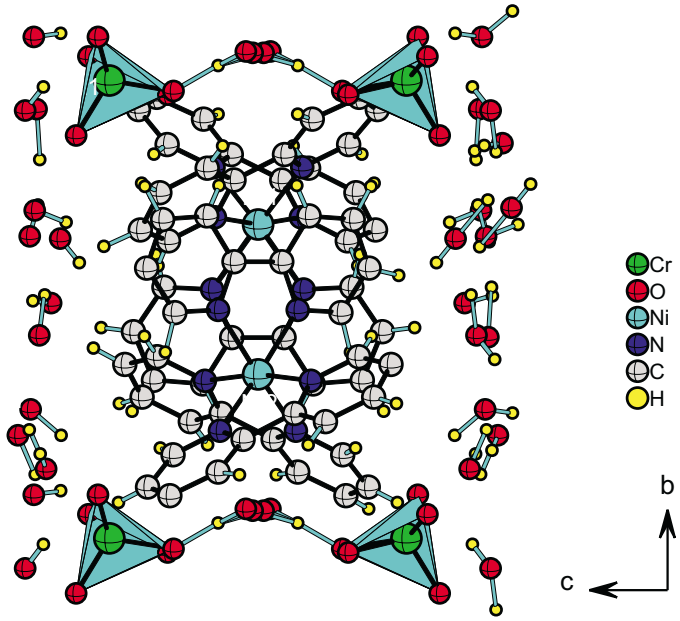

Figure 2. The hydrogen-bonded between chromate ions and a O(8) of water molecules in $[Ni(bpy)_3]CrO_4{\cdot}7.5H_2O$ (**1**).

The crystal structure of **2** consists of the complex $[Ni(bpy)_2(OCrO_3)(H_2O)]$ and five molecules of crystallization water. The Ni(II) ion has a distorted octahedral environment and is coordinated by four N atoms from two chelating bpy groups, one water O(1A) atom and O(1) atom of the CrO_4^{2-} anion (Fig. 3). The Ni–N_{bpy} distances (mean value 2.079(3) Å) similar to those found recently in polyanionic $[Ni(bpy)_2(H_2O)(PW_{12}O_{40})]^{3-}$ [31], are shorter than the Ni–O(1A) bond length (2.124(3) Å) but longer than the Ni–O(1) distance (2.046(3) Å) (Table 2). As illustrated in Fig. 3, the water molecules linked to the Ni(II) ion are hydrogen bonded to the O(3) and O(4) atoms of the neighboring chromate ions. The O(2) atom of the CrO_4^{2-} anion is hydrogen bonded to the water O(3A) atom.

Generally, the analysis of the crystal structure of the metal ion complexes with organic ligands, containing the chromate ion, shows three modes of arrangement of the CrO_4 entity: (i) – bidentate bridging $-O_2CrO_2-$ with symmetric [32–36] and asymmetric [37–40] metal–O(Cr) bonds (the pseudotetrahedral symmetry of the chromate moiety with two equal Cr–O bonds in the bridge was found in studied cases most); (ii) – bidentate chelating $-O_2CrO_2-$ [41] and (iii) – a combination of (i) and (ii) [41]. Monodentate chromate coordination (iv) in the complexes with organic ligand has already been recorded [42a–b]. Such cases were found in this work. The combination of (ii) and (iv) was found in simple $KLa(CrO_4)_2$ [42c–43]. Non-coordinate chromate should be expected in analogy to other tetrahedral anions like, *e.g.* ClO_4^- observed in various complexes [16,18,44–46].

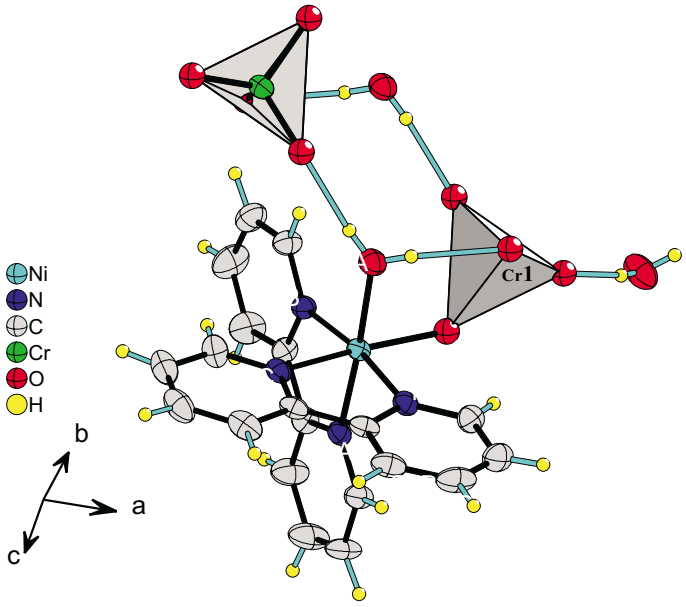

Figure 3. A perspective view of the coordination sphere of $[Ni(bpy)_2(OCrO_3)(H_2O)]$ in crystal **2**.

Infrared spectra: The infrared spectra of **1–3** are presented in Table 3 and Fig. 4. There are two main regions assigned to the CrO_4^{2-} entity: 780–950 cm^{-1} and 300–550 cm^{-1} [47]. In the 780–950 cm^{-1} region for tetrahedral symmetry, ν_3 should remain unsplit [48]. However, in **1** two small shoulders observed on ν_3 band (Fig. 4a) can be assigned to the dynamic disorder of the CrO_4 tetrahedron (see the structural part). For **2** and **3** the splitting of ν_3 are characteristic of the coordinated chromate ion [48–49]. According to the symmetry rules, on decreasing $T_d \rightarrow C_{3v} \rightarrow C_{2v}$, two and three components of ν_3 are found as expected, respectively (Fig. 4) [47]. In **2** and **3** a new band appearing at ~820 cm^{-1} and ~540 cm^{-1} were assigned to the ν_{as} and ν_s in the Ni–O–Cr bridge [49], respectively. Under the digital filtration process the asymmetric band at *ca.* 810–820 cm^{-1} assigned to the bridge splits into two well-separated bands (Fig. 4b and 4c). The higher transition energy was assigned to the bridge vibrations [49], whereas the other one was attributed to the rocking vibrations of the H_2O molecules [47] readily seen in **1** (Fig. 4a). As there is no structure of the complex **3**, the comparison of the mode splitting of the ν_3 and ν_4 bands between **1**, **2** and **3** suggests C_{2v} symmetry for the chromate entity in **3** (Chart 1) [47-48]. The C_{2v} symmetry of the chromate can be realized as a chelate or a bridge. As the bridging coordination is generally favored by the chromate ion [32,33,36,39,50], such coordination has been proposed for **3**. Moreover, the difference in the chromate coordination between **2** and **3** was confirmed through the shift and the change of the shape of the ν_{as} transition assigned to the Ni–O–Cr bridge.

Table 3. The most important vibrational frequencies (in cm^{-1}), band assignments and magnetic moments for **1–3**.

	ν(OH)	ν_{as}(Ni–O–Cr)	$\rho_r(H_2O)$	ν_{sym}(Ni–O–Cr)	$\nu(Ni–O_{H_2O})$	ν(Ni–N)	μ[BM] T = 297 K
1	3406_s	–	812_w	–	–	282_s 260_w	3.48 [19]
2	3386_s 3220_{sh}	818_m	810_m	545_m	443_w	264_s 257_s	3.28
3	3105_m	825_m	810_m	543_m	445_s	264_s 238_s	3.38 [19]

Electronic spectra: 8000–20000 cm^{-1} region: In this region two of low intensity bands related to the d-d (d^8) transitions [51] are observed (Table 4, Fig. 5, 6). In the spectra of **1–3**, the red shift of the band positions is connected with the systematic changes of the donor atom position in the spectrochemical series N_6, N_4O_2 and N_2O_4 [51]. The structure of the cationic part of **1** represents the known trigonally distorted octahedron (D_{3d}) [51–52], whereas the environment of **2** is a tetragonally distorted octahedron around Ni(II) ion (D_{4h}) [53]. However, as the respective splitting of the first two d-d bands, due to the $O_h \rightarrow C_{2V}$ symmetry lowering were not found, O_h (*i.e.* D_{3d}) has been applied for **1** and D_{4h} for **2–3**. The crystal field parameters calculated in D_{4h} model (Table 5) seem to be very reasonable.

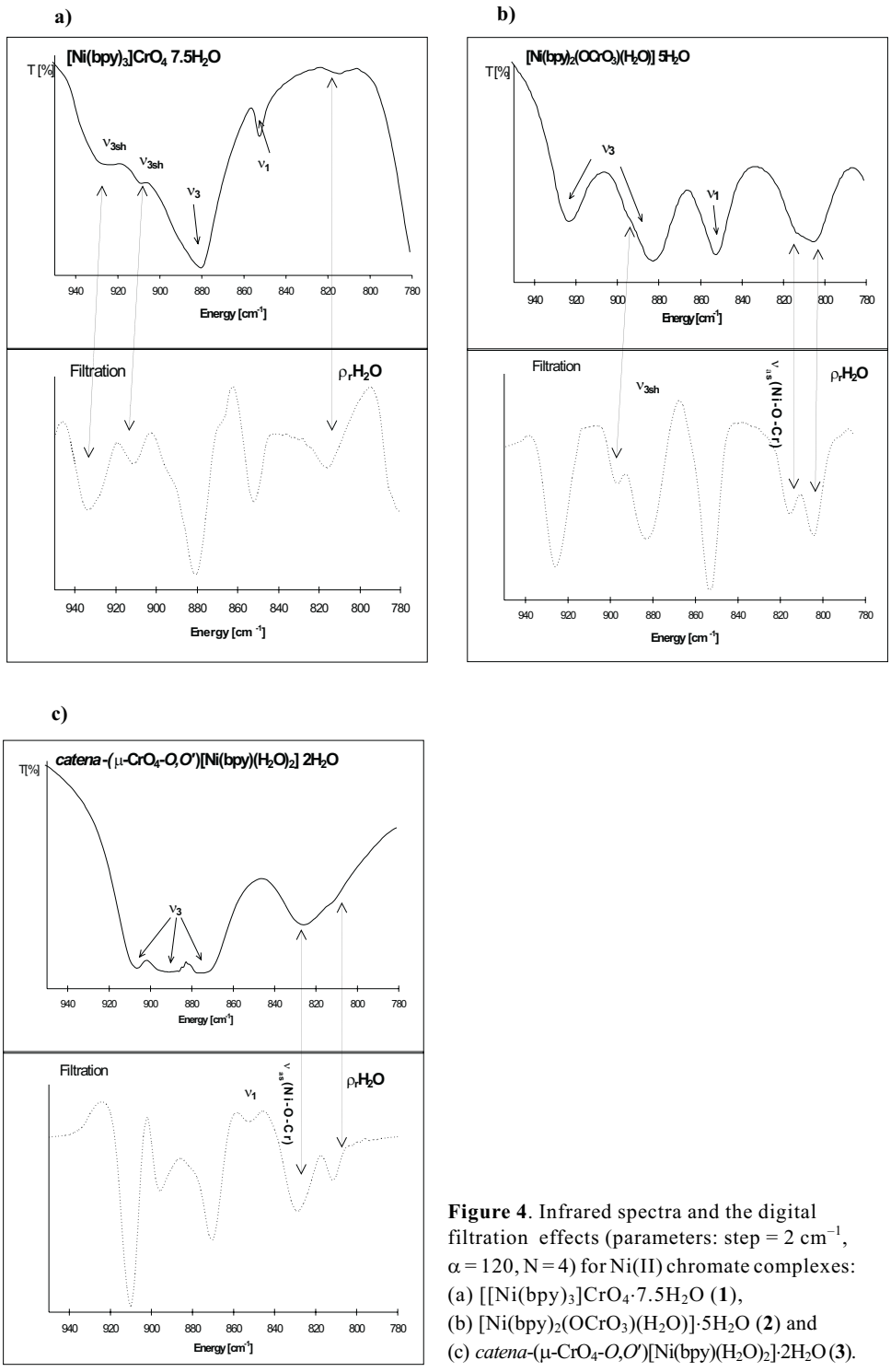

Figure 4. Infrared spectra and the digital filtration effects (parameters: step = 2 cm^{-1}, $\alpha = 120$, $N = 4$) for Ni(II) chromate complexes: (a) $[[Ni(bpy)_3]CrO_4 \cdot 7.5H_2O$ (**1**), (b) $[Ni(bpy)_2(OCrO_3)(H_2O)] \cdot 5H_2O$ (**2**) and (c) *catena*-(μ-CrO_4-*O*,*O'*)$[Ni(bpy)(H_2O)_2] \cdot 2H_2O$ (**3**).

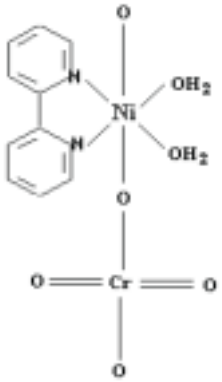

Chart 1. The coordination arrangement of *catena*-(μ-CrO_4-*O*,*O*′)[Ni(bpy)(H_2O)$_2$]·2H_2O (**3**).

Table 4. Band assignments for the deconvoluted electronic spectra of Ni(II) complexes (energy in cm^{-1}) in the 7000–30000 cm^{-1} region (molar absorption coefficients ε ($dm^3 \cdot mol^{-1} \cdot cm^{-1}$) in parentheses).

	Experimental conditions	Compounds [chromophore]					
		1 $[N_6]$[a]	**2** $[N^4O_2]$[b]		**3** $[N_2O_4]$[b]		$Ni(H_2O)_6^{2+}$ $[O_6]$[a]
	cryst. (293 K)	10045	12770				
^1E_g	cryst. (4 K)	9670	12810				
	refl.	10103	12850		13000		
	sn.	9610 (0.31)	12940 (0.98)				14355 (0.18)
	cryst. (293 K)	12705	10700[c]	11680[d]			
$^3T_{2g}$ **(F)**	cryst. (4 K)	13230	10880[c]	11530[d]			
	refl.	13130	10700[c]	11740[d]	8040[c]	10900[d]	
	sn.	12705 (9.14)	10630[c] (6.82)	11870[d] (2.22)			8560 (6.07)
Ni–O–Cr	cryst. (293 K)		14750				
	cryst. (4 K)		14250				
	refl.		15220		14000		
	sn.		15790 (0.88)				
	cryst. (293 K)	18640	16020[e]	17575[f]			
$^3T_{1g}$**(F)**	cryst. (4 K)	19080	16140[e]	17570[f]			
	refl.	18918	16120[e]	17710[f]	14550[*]	14550[*]	
	sn.	18355 (6.17)	16110[e] (2.67)	17630[f] (5.69)			14170 (2.87)
	cryst. (295 K)	20470[**]	20520[**]				
$^1T_{2g}$	cryst. (4 K)	20570[**]	20740[**]				
	refl.	20780[**]	20980[**]		21150[**]		
	sn.	20050[**]	21050**				22450 (0.27)
$^1A_1 \rightarrow {}^1T_1$[***]	refl.	22350, 23120, 23700	21200, 21960, 22900		21450, 21990, 22700		
	sn.	21460 (110), 22540 (130), 23320 (71)	21560 (95), 22610 (120), 23350 (60)				
$^1A_1 \rightarrow {}^1T_2$[***]	refl.	26950	26150		26100		
	sn.	27250 (1480)	27290 (1680)				

[a]O_h symmetry, [b]D_{4h} symmetry, [c] ^3E_g, [d] $^3B_{2g}$, [e] $^3A_{2g}$, [f] ^3E_g
[*]v_{0-0} energy, [**]position taken from the digital filtration (parameters: step = 30, α = 80, N = 10),
[***]CT O→Cr transitions.

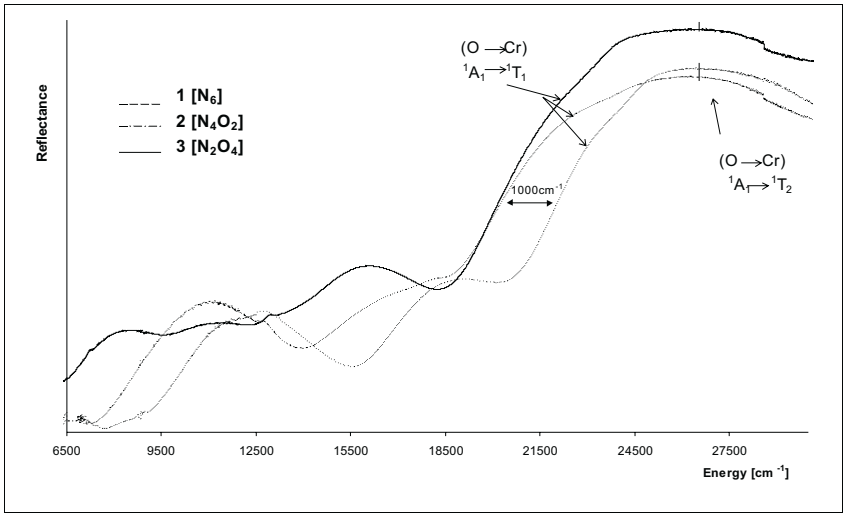

Figure 5. Reflectance spectra of $[Ni(bpy)_3]CrO_4 \cdot 7.5H_2O$ (**1**), $[Ni(bpy)_2(OCrO_3)(H_2O)] \cdot 5H_2O$ (**2**) and *catena*-(μ-CrO_4-*O*,*O*′)$[Ni(bpy)(H_2O)_2] \cdot 2H_2O$ (**3**).

The spectrum of **3** needs more comments. It is the compound, which is in the powder form of low solubility, thus the reflectance spectrum was the only subject of the analysis. Fortunately, the identical chromophore N_2O_4 was found in the crystals of $[Ni(phen)(OCrO_3)(H_2O)_3] \cdot H_2O$ [54]. Thus, the analysis of **3** was performed on the basis of the spectrum of this compound. In the spectra of both compounds the significant splitting (~2500 cm^{-1}) of the first d-d band is observed (in contrast to the second d-d band) (Table 4). The spectrum of phen complex exhibits an unsplit second d-d band with vibrational fine structure at 540 cm^{-1} [54]. Reasonable crystal field parameters (expecially Racah B parameter) were only obtained when the v_{0-0} (15150 cm^{-1}) was taken in the calculations as a second d-d band position (composed with $^3A_{2g}$ and ^3E_g) [54]. The same procedure was applied for compound **3**. Unfortunately, because of low resolution of its reflectance spectra, only traces of the respective vibronic structure were found, so that the v_{0-0} energy was approximated *via* phen complex [54]. In phen complex all bands are blue shifted in *ca.* 600 cm^{-1} in comparison with **3**, therefore, 14550 cm^{-1} as v_{0-0} of the second d-d band was proposed for **3**.

The electronic spectra of the complexes studied in various environments were resolved into the component bands (Table 4, Fig. 6). The number of the bands, taken in the analysis, was the consequence of (a) – the spin-orbit interaction (O_h symmetry) and (b) – predictions of the crystal field theory [28–29]. Mathematically (assuming that the $^3B_{2g}$ state possesses a higher energy than the ^3E_g state) based on energy matrices [28–29], from first four energies of the d-d spin-allowed transition, one obtains two sets of possible parameters. For example, for **2** in formamide (Tab. 4) the following solutions have been obtained:

	^3E_g	$^3B_{2g}$	$^3A_{2g}$	^3E_g	Dq	B	Ds	Dt
(i)	10630	11870	17630	16110	1187	632	425	–140
(ii)	10630	11870	16110	17630	1187	703	–365	–130

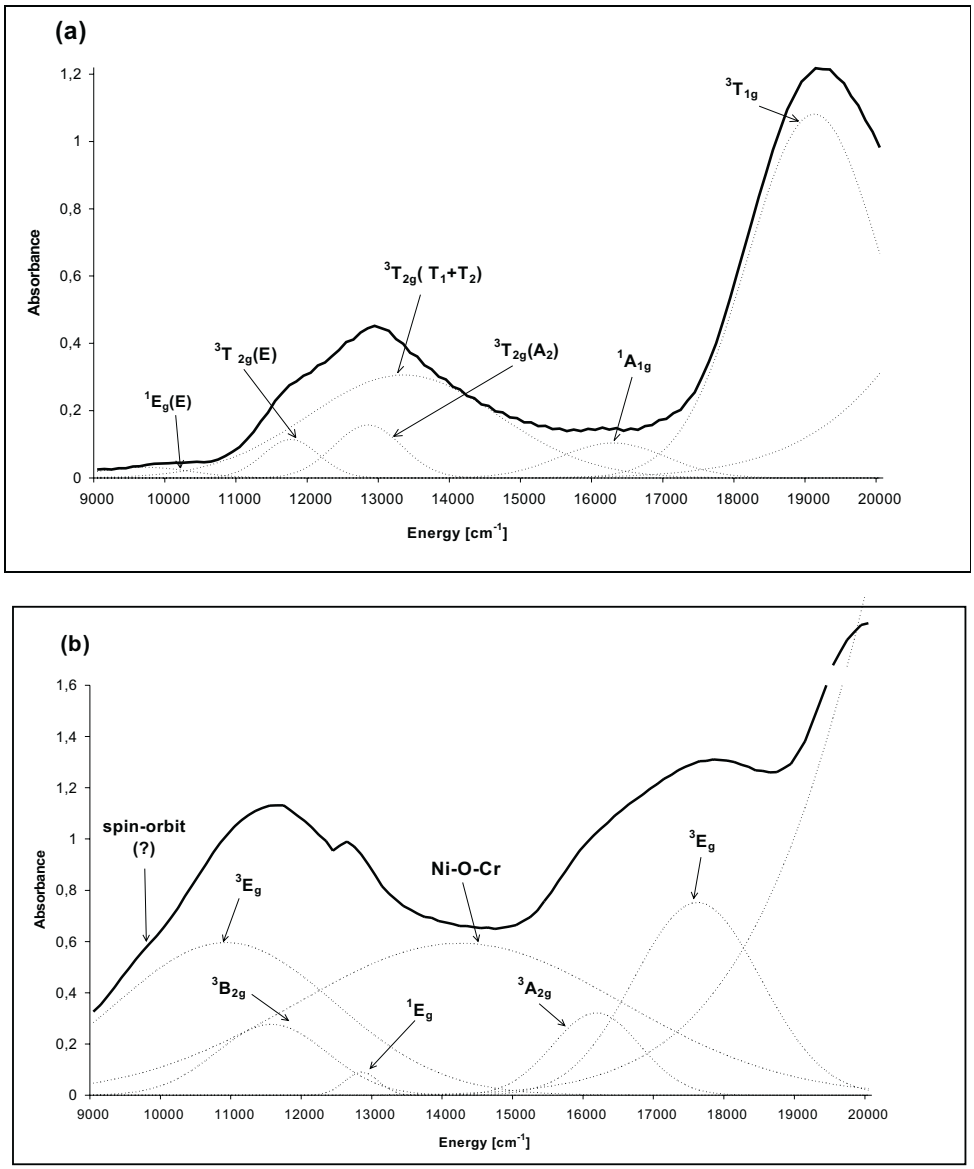

Figure 6. Low-temperature (4 K) single crystal electronic absorption spectra of (a) $[Ni(bpy)_3]CrO_4 \cdot 7.5H_2O$ (**1**) and (b) $[Ni(bpy)_2(OCrO_3)(H_2O)] \cdot 5H_2O$ (**2**).

For both sets the Dq parameter is equal, Dt is acceptable and Ds parameter is not very informative, thus only the value of B parameter may be taken as a criterion of choice. For set (i) its value is very similar to the respective value for **1** (Table 6), which is not acceptable. Only the value of B for set (ii) well describes the changes in **1**–**3** and $[Ni(H_2O)_6]^{2+}$ (N_6, N_4O_2, N_2O_4 and O_6). A similar discussion is valid also for other compounds.

Table 5. Ligand field parameters for nickel(II) chromate complexes (cm^{-1}).

	Experimental conditions	compound [chromophore]			
		1 [N_6]	**2** [N_4O_2]	**3** [N_2O_4]	$Ni(H_2O)^{2+}[O_6]$
Dq	cryst. (293 K)	1270	1168		
	cryst. (4 K)	1323	1153		
	refl.	1313	1174	1090	
	sn.	1271	1186		856
B	cryst. (293 K)	634	697		
	cryst. (4 K)	609	693		
	refl.	601	718	820	
	sn.	589	703		892
Ds	cryst. (293 K)		–375		
	cryst. (4 K)		–350		
	refl.		–380	282	
	sn.		–365		
Dt	cryst. (293 K)		–100		
	cryst. (4 K)		–70		
	refl.		–110	–326	
	sn.		–130		

Spin-orbit mixing effect: The characteristic feature of the d-d region for the spectra of the nickel(II) ion is the presence of the double-humped band at *ca.* 10000–16000 cm^{-1}, assigned in the O_h symmetry to the $^3A_{2g}\rightarrow{}^3T_{1g}$ transition (the second spin allowed transition *e.g.* $[Ni(H_2O)_6]^{2+}$) [55] or to the $^3A_{2g}\rightarrow{}^3T_{2g}$ (the first spin allowed transition, *e.g.* $[Ni(en)_3]^{2+}$) [51,52,56]. The shape of the band is explained as a result of spin-orbit interaction between ^1E_g and $^3T_{1g}$ or $^3T_{2g}$ states [56e–f]. The $^3T_{2g}$ state comprises $E+T_1+T_2+A_2$ spin-orbit level, the $^3T_{1g}$ state comprises $A_1+T_1+T_2+E$ spin-orbit levels, whereas ^1E_g state (spin forbidden) consists of one E spin-orbit level. Therefore, the E spin-orbit levels for $^3T_{1g}$ or $^3T_{2g}$ and ^1E_g may interact [56e–f]. As results of the spin-orbit mixing, the normally weak and sharp bands associated with spin forbidden transition broaden and become stronger, whereas the spin-orbit levels E associated with spin allowed transitions lose intensity and become narrower. Thus, narrow components appear on the spectral contour as new bands. In the system studied such band was found at *ca.* 11700 cm^{-1} ($^3T_{2g}$(E), Fig. 6) and 15050 cm^{-1} ($^3T_{1g}$(E)) for **1** and $[Ni(H_2O)_6]^{2+}$, respectively. The ''fading'' of the spin-orbit components leads to the band asymmetry of the spin-allowed transition ($^3T_{2g}$ and $^3T_{1g}$ for **1** and $[Ni(H_2O)_6]^{2+}$, respectively). The consequence of this asymmetry is an erroneous fitting of the band positions and consequently, a miscalculation of the crystal field parameters. To solve this problem the following steps have been applied:

1) Deconvolution of the band assigned to spin allowed transition, which was earlier divided into two groups. The first one represented by broad spin-orbit components T_1, T_2 and the second one by narrow components A_1 or A_2. In this case (the Ni(II) core in **1** and $[Ni(H_2O)_6]^{2+}$), there are T_1, T_2 levels (from $^3T_{2g}$ or $^3T_{1g}$) and A_2 (from $^3T_{2g}$) or A_1 (from $^3T_{1g}$) levels, for broad and narrow, respectively.

2) Calculation of the real band position of the spin allowed transitions as weighted average of the positions of the broad and narrow components with the weight of the fields under the band curves proportional to the oscillator strength.

The validity of this approach for spectra of **1** and $[Ni(H_2O)_6]^{2+}$ has been confirmed by the reasonable magnitudes of the crystal field parameters obtained for the systems (Table 5). One can also enquire the spin-orbit effect for the D_{4h} symmetry (Fig. 6b). In this case the spin allowed $^3T_{2g}$ state splits into ^3E_g and $^3B_{2g}$ and spin forbidden ^1E_g state splits into $^1A_{1g}$ and $^1B_{1g}$. The ^3E_g state comprises $A_1+A_2+E+B_1+B_2$ spin-orbit levels, whereas $^3B_{2g}$ state relates to $E+B_1$ [29]. As a $^1B_{1g}$ state consists of only one B_1 spin-orbit level such a level may interact with the B_1 states derived from various products of low symmetry splitting: ^3E_g ($^3T_{2g}$) and $^3B_{2g}$ ($^3T_{2g}$). The $^1A_{1g}$ component of ^1E_g comprises only one spin-orbit level A_1 and may interact with A_1 spin-orbit level from ^3E_g. The detailed analysis of **2** spectra (for **3** only less informative reflectance spectrum was measured) allowed to find the possible candidates to the spin-orbit bands (especially at *ca.* 9500 cm^{-1} (**2**) – see Fig. 6b – which can be assigned, according to the discussion presented above to the ^3E_g (A_1). However, we did not decide to take them into account in the deconvolution process. The existence of several peaks under one broad peak could be questionable. However, the results of Gaussian analysis of the spectra of **2** and **3** even without taking the spin-orbit mixing effect into account are rationable (Table 4) and crystal field parameters (Table 5) calculated based on this analysis well fit to the whole system. Generally, the data show the stability of the [Ni(II)-(2,2′-bpy)-CrO_4^{2-}] system. For various techniques used, various phases and temperatures, the regularity of the changes for all energy transitions and calculated parameters is remarkable.

The transition due to the bridge: In contrast to the infrared data, the problem of the electronic transitions, assigned to the bridge in the polynuclear species, has been very rarely discussed [33,57]. An attempt to assign the LMCT band, due to the bridge, was done by Oshio *et al.* [33]. However, their assignment of the Ni–O transition in the Ni–O–Cr bridge seems not to be correct. A strong absorption band (~24000 cm^{-1}) with a shoulder (~19600 cm^{-1}) was observed in the Ni(II) chromate complex with the cyclam ligand. The higher energy band was assigned to LMCT O→Cr [71–73], whereas the lower one was assigned to LMCT (O→Ni) in the bridge. However, as the energy difference between the transitions is approximately the difference between the respective energies in the trigonally distorted CrO_4^{2-} entity [59], the shoulder could rather be related to the lowering symmetry effect in the coordinated chromate ion with both energies shifted to the red [58,60b]. In the deconvoluted spectra of **2** and **3**, one additional broad band (in 4 K half width *ca.* 3000 cm^{-1}) was found at *ca.* 14500 cm^{-1} of intensity comparable to the d-d bands (Fig. 6b). Its possible origin can be due to one of the following: (a) – the band component of the symmetry lowering ($D_{4h}\rightarrow C_{2v}$), (b) – the spin forbidden transitions in the chromate ion [58], (c) – the transition due to the Ni–O–Cr bridge. (a) was rejected, because the calculation showed that in such a case the magnitude of the covalency (Racah B parameter) for **1** and **2** would be of comparable value (*ca.* 600 cm^{-1}), which is not acceptable. In our opinion,

both (b) and (c) are acceptable. However, (b) may be less probable, because of the absence of this band in **1**. Thus, we are rather inclined to the interpretation that the band at ~15000 cm^{-1} can be assigned to the O→Ni or O→Cr transition in the Ni–O–Cr bridge. The low intensity of the band suggests multiple forbidness of the transition [24].

20000–30000 cm^{-1} region: In this region the dominating feature is the presence of the strong *ca*. 27000 cm^{-1} CT band assigned to the $^1A_1 \rightarrow {}^1T_2$ ($t_1 \rightarrow 2e$) (T_d) transition in the chromate ion [52,58–60]. Additionally, in all compounds and environments the shoulder at *ca.* 21000–23000 cm^{-1} has been observed (Fig. 4). In the literature this shoulder was assigned to the symmetry forbidden $^1A_1 \rightarrow {}^1T_1$ (T_d) [58,60] in free chromate or to the symmetry lowering component $T_d \rightarrow C_{3v}$ or C_{2v} (^1E) in the mono substituted chromate ion and the dichromate [59], respectively. In both cases the energies of the levels were found to be roughly the same [58,59a]. The difference in the chromate ion position between **1** on the one hand and **2–3** on the other have been observed in this *ca.* 21000–23000 cm^{-1} region only in the reflectance spectra (Table 4, Fig. 5). For the latter red shift of 1000 cm^{-1} has been observed. Thus we suggested the different origin of this band in the solid state, *i.e.* for **1** it is spin allowed $^1A_1 \rightarrow {}^1T_1$ transition, whereas for **2–3** it can be an effect of the symmetry lowering. This difference indicates not only the change of the respective level due to the symmetry decreasing but also its lowering.

Supporting information available: Supplementary data are available from CCDC, 12 Union Road, Cambridge CB2 1EZ, on request, quoting the deposition number 153709 and 153710.

Acknowledgments

The authors thank Prof. W. Wojciechowski for a generous gift of helium. We are also indebted to Dr. S. Gołąb and Dr. J. Sokolnicki for invaluable help in the cryogenic experiments. We would like to thank the Wrocław University of Technology (Grant No. 342117) and Polish State Committee for Scientific Research (Grant No. 3T09A 09218) for financial support.

REFERENCES

1. Zhitkovich A., Voikun V. and Costa M., *Carcinogenesis* **16**, 907 (1995).
2. Cieślak-Golonka M., *Polyhedron Report*, **15**, 3667 (1996).
3. Stearns D.E. and Wetterhahn K.E., NATO ASI 1997 Series *26*, 15 and the references therein.
4. Perez-Benito J.F. and Arias C., *J. Phys. Chem.*, **A102**, 5837 (1998).
5. Codd R. and Lay P.A., *J. Am. Chem. Soc.*, **121**, 7864 (1999).
6. Szyba K., Cieślak-Golonka M. and Gąsiorowski K., *BioMetals*, **5**, 157 (1992).
7. Gąsiorowski K., Szyba K., Woźniak D., Cieślak-Golonka M. and Rzepka-Materny M., *BioMetals*, **11**, 175 (1998), and the references therein.
8. Stanica N., Stager C.V., Cimpoesu M. and Andruh M., *Polyhedron*, **17**, 1787 (1998).
9. Shi J.M., Cui J.Z., Liao D.Z., Miao M.M., Liu Y.J., Jiang Z.H. and Wang G.L., *Polish J. Chem.,* **72**, 643 (1998).
10. Garnovskii A.D., Burlov A.S., Garnovskii D.A., Vasilchenko I.S, Antsichkina A.S., Sadikov G.G., Sousa A., Garcia-Vazquez J.A., Romero J., Duran M.L., Sousa-Pedrares A. and Gomez C., *Polyhedron*, **18**, 863 (1999).

11. Gosmini C., Lasry S., Nedelec J.Y. and Perichon J., *Tetrahedron*, **54**, 1289 (1998).
12. Hayashi Y., Mano H. and Uehara A., *Chem. Lett.*, 899 (1998).
13. Zeki Y.S., Nedim M.M., Nuras T. and Yasar G., *Acta Chem. Scand.*, **52**, 694 (1998).
14. Ye B.H., Chen X.M., Xue G.Q. and Ji L.N., *J. Chem. Soc., Dalton Trans.*, 2827 (1998).
15. Plater M.J., Foreman M.R.St.J., Coronado E., Gomez-Garcia C.J. and Slawin A.M.Z., *J. Chem. Soc., Dalton Trans.*, 4209 (1999).
16. Pavlishchuk W.W., Kalaida A.W. and Goreshnik E.A., *Koord. Khim.*, **25**, 542 (1999) (in Russian).
17. Molina-Svendsen H., Bojesen G. and McKenzie Ch.J., *Inorg. Chem.*, **37**, 1981 (1998).
18. Ye B.H., Xue F., Xue G.Q., Ji L.N. and Mak T.C.W., *Polyhedron*, **18**, 1785 (1999).
19. Repka A., Cieślak-Golonka M., Surga W. and Żurowski K., *Thermochim. Acta*, **313**, 9 (1998).
20. Sheldrick G.M., SHELXL-97, Programs for the Solution and the Refinement of Crystal Structures from Diffraction Data. University of Gottingen, 1997.
21. Bierman G. and Ziegler H., *Anal. Chem.*, **58**, 536 (1986).
22. Myrczek J., *Spectr. Lett*., **23**, 1027 (1990).
23. Cieślak-Golonka M., Raczko M. and Staszak Z., *Polyhedron*, **11**, 2549 (1992).
24. Wojciechowska A., Staszak Z., Pietraszko A., Bronowska W. and Cieślak-Golonka M., *Polyhedron*, **21**, 2063 (2001).
25. Slavič I.A., *Nucl. Instr. Meth.*, **134**, 285 (1976).
26. Bartecki A. and Staszak Z., *Comp. Enh. Spectr.*, **2**, 129 (1984).
27. Miernik D., Arkowska A., Grażyńska E. and Staszak Z., *Spectr. Lett*., **24**, 371 (1991).
28. Perumareddi J.R., *J. Phys. Chem.*, **76**, 3401 (1972).
29. Merriam J.S. and Perumareddi J.R., *J. Phys. Chem*., **79**, 142 (1975).
30. Wada A., Sakebe N. and Tanaka J., *Acta Cryst*., **B32**, 1121 (1976).
31. Xu Y., Xu J.Q., Zhang K.L., Zhang Y. and You X.Z., *Chem. Commun.*, 153 (2000).
32. Oshio H., Kikuchi T., Kikuchi K. and Ito T., *Mol. Cryst. Liq. Cryst.*, **305**, 23 (1997).
33. Oshio H., Okamoto H., Kikuchi T. and Ito T., *Inorg. Chem.*, **36**, 3201 (1997).
34. Harel M., Knobler C. and McCullough J.D., *Inorg. Chem.*, **8**, 11 (1969).
35. Bensch W., Seferiadis N. and Oswald H.R., *Inorg. Chim. Acta*, **126**, 113 (1987).
36. Oshio H., Kikuchi T. and Ito T., *Inorg. Chem.*, **35**, 4938 (1996).
37. Choi K.Y., Park J.R. and Suh I.H., *Polyhedron*, **18**, 497 (1998).
38. Choi K.Y., Suh I.H. and Kim D.W., *Inorg. Chim. Acta*, **293**, 100 (1999).
39. Gatehouse B.M. and Guddat L.W., *Acta Cryst.*, **C43**, 1445 (1987).
40. Drüeke S., Wieghardt K., Nuber B., Weiss J., Fleischhauer H.P., Gehring S. and Hasse W., *J. Am. Chem. Soc*., **111**, 8622 (1989).
41. Benetollo F., Bombieri G., Gilli P., Harlow P.M., Polo A. and Vallarino L.M., *Polyhedron*, **14**, 2255 (1995).
42. (a) Bruggemann R.C. and Thewalt U., *Z. Naturforsch B*, **49**, 1531 (1994); (b) Allen J.L., Shapley P.A. and Wilson S.R., *Organometallics*, **13**, 3749 (1994); (c)Bueno I., Parada C., Garcia O., Puebla G.E., Monge A. and Ruiz-Valero C., *J. Chem. Soc., Dalton Trans.*, 1911 (1988).
43. Leppä - aho J., *Acta Cryst*., **C50**, 663 (1994).
44. Tedenac J.C. and Philippot E., *Acta Cryst.*, **B30**, 2286 (1974).
45. Liu Z.M., Jiang Z.H., Liao D.Z. and Wang G.L., *Polyhedron*, **10**, 101 (1991).
46. Rodriguez-Martin Y., Gonzalez-Platas J. and Ruiz-Perez C., *Acta Cryst.*, **C55**, 1087 (1999).
47. Nakamoto K., *Infrared and Ramana Spectra of Inorganic and Coordination Compounds*, A Wiley-Interscience Pub. John Wiley & Sons, Inc, 5th ed. 1997.
48. Hathaway B.J., in: *Compreh. Coord. Chem*., Pergamon Press, Oxford 1987, Vol. **2**.
49. Cieślak-Golonka M., *Coord. Chem. Rev.*, **109**, 223 (1991), and the references therein.
50. Gili P. and Lorenzo-Luis P.A., *Coord. Chem. Rev.*, **193–195**, 747 (1999), and the references therein.
51. Lever A.B.P., *Inorganic Electronic Spectroscopy*, Elsevier Press: NY, 2nd ed. 1984.
52. Palmer R.A. and Piper T.S., *Inorg. Chem.*, **5**, 864 (1966).
53. Bunel S., Gil L., Moraga E. and Bobadilla H., *Inorg. Chim. Acta*, **4:3**, 415 (1970).
54. Bronowska W., Pietraszko A., Daszkiewicz M., Staszak Z., Cieślak-Golonka M. and Wojciechowska A., submitted to *Polyhedron.*
55. Solomon E.I. and Ballhausen C., *J. Mol. Phys.*, **29**, 279 (1975).

56. (a) Dingle R. and Palmer R.A., *Theor. Chim. Acta*, **6**, 249 (1966). (b) Zompa L.J., *Inorg. Chem*., **17**, 2531 (1978). (c) Hart S.M., Boeyens J.C.A. and Hancock R.D., *Inorg. Chem*., **22**, 982 (1983). (d) Martin L.L., Martin R.L., Murray K.S. and Sargeson A.M., *Inorg. Chem.*, **29**, 1387 (1990). (e) Stranger R., Wallis S.C., Gahan L.R., Kennard C.H. and Byriel K.A., *J. Chem. Soc., Dalt. Trans.*, 297 (1992). (f) Stranger R., McMahon K.L., Gahan L.R., Bruce J.I. and Hambley T.W., *Inorg. Chem.*, **36**, 3466 (1997).
57. Stawińska J., Staszak Z., Jezierska J., Cieślak-Golonka M. and Daszkiewicz M., *Polish J. Chem.*, **74**, 291 (2000).
58. Tłaczała T., Cieślak-Golonka M., Bartecki A. and Raczko M., *Appl. Spectr.*, **47**, 1704 (1993).
59. (a) Miskowski V., Gray B.H. and Ballhausen C.J., *Mol. Phys*., **28**, 729 (1974), and the references therein. (b) Hog J.H., Ballhausen C.J. and Solomon E.I., *Mol. Phys*., **32**, 807 (1976).
60. (a) Johnson L.W. and McGlynn S.P., *Chem. Phys. Lett*., **7**, 618 (1970). (b) Robbins D.J. and Day P., *Mol. Phys*., **34**, 893 (1972).